BJRS

BRAZILIAN JOURNAL
OF
RADIATION SCIENCES
10-02A (2022) 01-11

Dosimetric evaluation of breast radiotherapy treatments in the presence of magnetic valve expansion prostheses

Lizar[1] J.C., Krutman[2] Y., Pavoni[1] J.F., Baffa[1] O.

[1] Departmento de Física, Faculdade de Filosofia, Ciências e Letras de Ribeirão Preto, Universidade de São Paulo, 14040-901 Ribeirão Preto, SP, Brazil. jclizar@usp.br

[2] Radiotherapy Department, Institute of Oncology, Soroka University Medical Center, Beer-Sheva 84100, Israel

ABSTRACT

This work intends to verify the influence on the dose distribution that the expansive prosthesis (SILIMED/470), containing a magnetic valve, generates in postoperative radiotherapy treatments of patients who underwent a mastectomy. The presence of this metal complicates the treatment planning stage due to the artifacts generated by the magnet in the acquisition of computed tomography. Radiochromic films (Gafchromic EBT2) were used for dose measurements inside the prosthesis, around the metal in a plastic phantom that simulates the breast geometry filled with water. An insert in the center allowed the placement of the magnet and 2.5 mm thick acrylic layers for film positioning above and below the metal at different depths. The phantom was irradiated according to a conformal radiotherapy planning performed in XiO software (CMS RTP) with no heterogeneity correction, using photon beams of 6 MV and 15 MV from the Oncor linear accelerator (Siemens) with a prescribed dose of 2 Gy. A film calibration methodology was performed, and the optical densities of the films were measured using a CQ-01 digital densitometer (MRA). For the 6MV irradiation, an overdose of 4.57% was obtained for all films, and, just above the magnet, an increase of 11.22% was noted. For the 15 MV beam, the films around the magnet had a dose increase of 8.60% considering the TPS value and 5 mm away from the metal, a decrease of 3.31% of the expected dose was observed.

Keywords: **radiation oncology, film dosimetry, mastectomy.**

ISSN: 2319-0612
DOI: https://doi.org/10.15392/bjrs.v10i2A.2014
Submitted: 2022-02-14
Accepted: 2022-07-07

1. INTRODUCTION

Breast cancer is the world's most prevalent cancer, other than non-melanoma skin cancer [1]. The non-metastatic breast cancer therapy consists of surgical resection and sampling or removal of axillary lymph nodes, considering postoperative radiation. Systemic therapy may be preoperative, postoperative, or both [2]. There are two main types of breast cancer surgery, a total mastectomy, or a lumpectomy. Reconstructive surgery can follow the mastectomy to recreate a breast, resulting in esthetical and psychosocial improvements for these patients [3]. The two-stage breast reconstruction is a common procedure among surgical reconstruction options. In this process, temporary implantation of an expansive prosthesis occurs first. The valve in the prosthesis has a magnet that guides the surgeon where to inject small volumes of saline solutions to slowly create a cavity that will later be filled with a permanent prosthesis. However, for these patients, post-mastectomy radiation therapy can improve survival and loco-regional control [4]. The expansive prosthesis metallic magnet presence during radiotherapy generates artifacts in the computed tomography (CT) images, making the target volumes delineation for the treatment planning difficult. The dose distribution calculation during the planning may also be influenced by the presence of the high atomic number (Z) metal in the magnet, once its CT number may be out of the usual range of the curve used for the conversion of CT numbers to electron densities in the treatment planning system. This study aims to verify the influence on the dose distribution that the expansive prosthesis (SILIMED/470), containing a magnetic valve, generates in postoperative radiotherapy treatments. With an experimental set up relatively simple it was possible to get robust results showing the importance of including the metal.

2. MATERIALS AND METHODS

2.1. Phantom

The magnetic valve from a SILIMED/470 prosthesis was separated from the prosthesis and used in this study. The magnetic valve (17.9 mm wide by 3.9 mm thick), made of titanium (Ti, density = 4.50 g/cm3) and samarium-cobalt magnet (SmCo5, d = 8.20–8.50 g/cm3), the titanium foil covers

the magnet to add extra protection. A plastic conical phantom (Tupperware®) simulating the breast shape was used. An opening was made in its center for the insertion of an acrylic cylindrical support with the magnet and 2.5 mm thick acrylic layers. This insert allows the radiochromic films positioning above and below the metal at three different depths, as illustrated in Figure 1-a. Figure 1-b details the metal, films, and acrylic layers' positioning. The films used in the phantom were cut in a circular shape with 2.3 cm diameter, corresponding to the insert diameter. The complete phantom is presented in Figure 1-c with the insert positioned inside it. It is possible to see that the metal magnet was located approximately in the middle of the simulated breast. During all the experiments, the phantom is filled with water to guarantee its tissue equivalence.

Figure 1: a) Phantom with the central hole for the insert. **b)** A close view of the insert with the rare earth metal magnet, the films and three acrylic disks of 2.5 mm on its the bottom. c) Complete phantom view with the insert in its positioning.

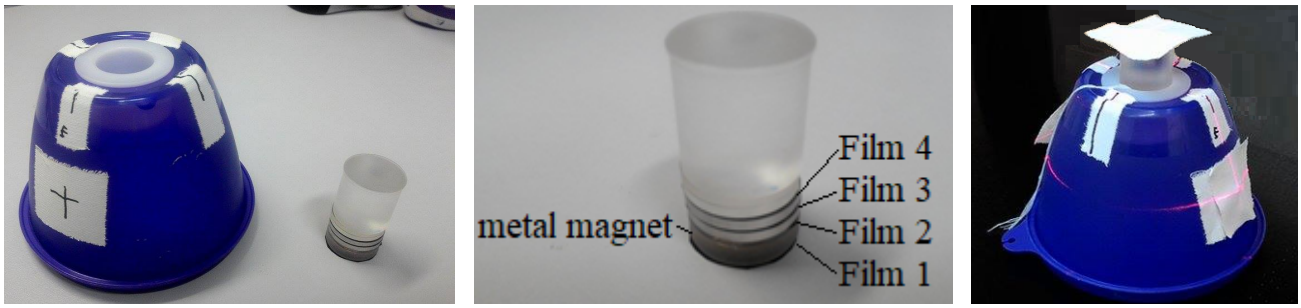

(a) (b) (c)

2.2. Treatment planning

The planning started with the phantom CT-Scanning (Brilliance CT Big Bore Radiology, Philips, Netherlands). At this step, the phantom was positioned on 5 cm of acrylic layers to guarantee backscattering during irradiation. Also, the metal magnet was not positioned in it to not generate artifacts in the images and avoid problems with the CT number to electron density table conversion. An acrylic layer replaced it with the exact dimensions.

The phantom images were sent to the XiO treatment planning system (Elekta Medical Systems, United Kingdom). The phantom volume was delineated as the planning target volume (PTV). Two treatment plans using two tangential and opposed beams were done (Figure 2), the first one using a

6 MV beam and the second a 15 MV beam, both from an Oncor Linear Accelerator (Siemens healthcare, Germany). The prescribed dose was 2 Gy and the plan was designed to deliver at least 90% of the prescribed dose to 90% of the PTV. No hot spot or high-dose variations at the future position of the films were allowed in the final plans. No heterogeneity corrections were employed in the dose calculations because, as stated before, the metal magnet was removed from the phantom at the CT images acquisition. This way, the measured dose values were compared with the TPS data (without heterogeneity corrections), providing the metal's real influence without the extra uncertainties that could be associated with the calculation algorithm [5,6].

Figure 2: Irradiation setup used for both energy irradiations. The phantom was positioned on the top of 5 cm of acrylic layers. The insert is also illustrated; the black material corresponds to the metal magnet and the yellow lines to the radiochromic films. The two tangential and opposed radiation beams are also presented. The zoomed part of the figure illustrates the dimensions of the region with the film and the metal port where the measurements were performed.

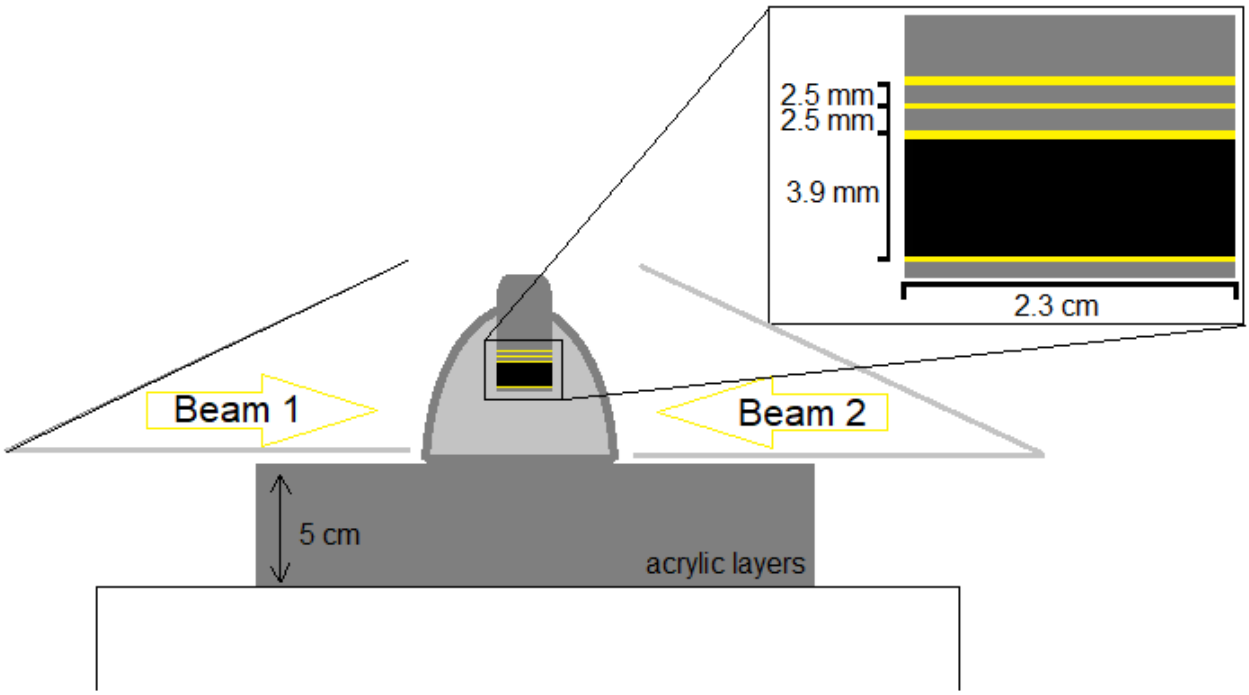

2.3. Radiochromic film dosimetry

The radiochromic film dosimetry was conducted using Gafchromic EBT2 films. Films with 3 x 3 cm^2 of area were irradiated using known doses (0 cGy, 50 cGy, 100 cGy, 150 cGy, 200 cGy, 250 cGy and 300 cGy) to achieve the calibration curve of the radiochromic film batch used. These patches were positioned at the depth of maximum dose in a cubic solid water phantom. A source to the surface distance of 100 cm and a field size of 20 x 20 cm^2 were used for irradiating the films with the known doses. This calibration methodology was repeated for both beam energies.

The dose readings were always done at least 24 hours after irradiation. The films' optical densities (OD) were measured using a digital densitometer CQ-01 (MRA, Brazil) with a pinhole diameter of 2 mm. Before using the densitometer, it was turned on and allowed to thermal stabilize for at least five minutes. The instrument was factory calibrated with an accuracy of ± 0.02 OD. The net OD was calculated for all films by subtracting the background OD value from the measured OD. Five net OD measurements were made (one in the center of the film, one above it, one below it, one in its left side, and other in its right side). The data presented are the average values with the standard deviation.

2.4. Irradiations

The phantom irradiation was done following the treatment plans described before. For the procedure, the metal magnet was used in the phantom insert, replacing the acrylic layer used for the CT acquisition, and the films evaluated in this study were also positioned on the phantom. Firstly, the 6 MV beam planning was delivered to the phantom, and the irradiated films were separated. After, new films were positioned in the phantom, and the 15 MV beam planning was delivered.

3. RESULTS AND DISCUSSION

The irradiated calibration films for both energies are shown in Figure 3, and their nonlinear responses as a function of dose are presented in Figure 4 for 6 MV and 15 MV beams. A curve fitting was done using a cubic polynomial function on both data, according to equation 1, and the fitting parameters are shown in Table 1.

$$Y = A + B.x + C.x^2 + D.x^3 \quad (1)$$

Figure 3: a) Calibration films irradiated with 6MV. **b)** Calibration films irradiated with 15 MV. The area of the film patches is 3 x 3 $cm^{2,}$ and the films are presented in ascending order of doses from 0 to 500 cGy.

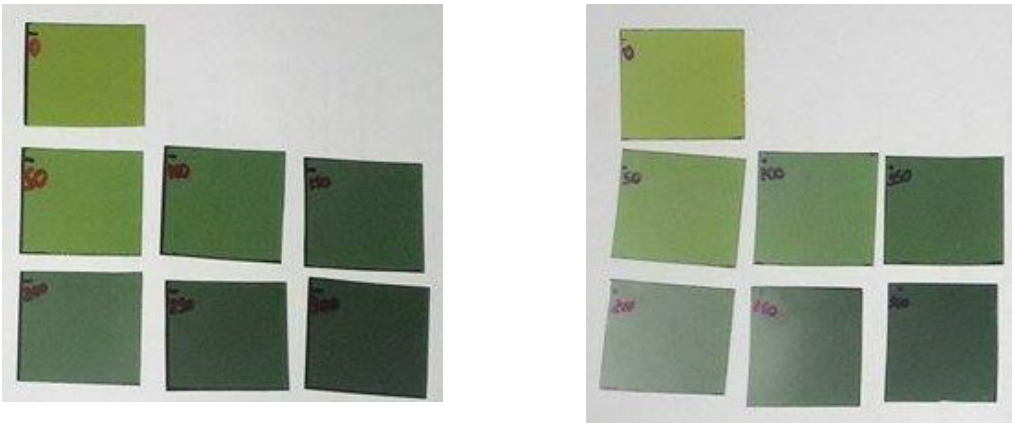

(a) (b)

Figure 4: Dose-response data relating net OD to dose with a third-order polynomial function fitting the points for the films irradiated with 6 MV and 15 MV.

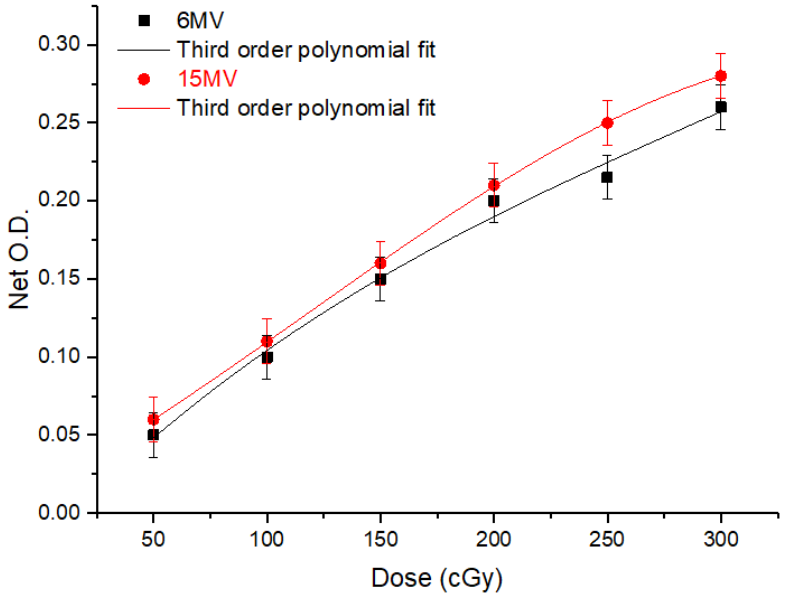

Table 1: Dose-response data relating DO to cubic polynomial function fitting parameters for the films irradiated with 6 MV and 15 MV.

Parameters	6 MV	15 MV
	Values	Values
A	-0.02 ± 0.04	0.017 ± 0.003
B	0.002 ± 8.6820E-4	7.775E-4 ± 0.7320E-4
C	-2.928E-6 ± 5.555E-6	2.111E-6 ± 0.468E-6
D	3.333E-9 ± 1.049E-8	-5.926E-9 ± 0.885E-10

The measured and the TPS expected doses for the four films used between the acrylic interfaces for 6 MV and 15 MV are presented in Table 2. The film positioning follows the Figure 1-b representation, with the first layer behind the magnet. The values in Table 2 were corrected considering the linear accelerator radiation daily output constancy of 0.48% for the 6 MV beam and 0.33% for the 15 MV beam.

Table 2: Measured and expected doses of the films irradiated in different positions for both energies evaluated.

	6 MV		15 MV	
Film Position	**Measured dose (cGy)**	**TPS dose (cGy)**	**Measured dose (cGy)**	**TPS dose (cGy)**
1	213.32 ± 5.80	204.00 ± 2.00	226.44 ± 5.88	208.50 ± 0.50
2	226.90± 5.80	204.00 ± 2.00	226.44 ± 5.88	208.50 ± 0.50
3	213.32 ± 5.80	204.00 ± 2.00	226,44 ± 5.88	208.50 ± 0.50
4	213.32 ± 5.80	204.00 ± 2.00	201.59 ± 5.88	208.50 ± 0.50

The absorbed doses measured by the films during the phantom irradiations were defined accordingly to the film calibration curve. These values were compared to the TPS expected doses calculated by the treatment plan at the same positions. Considering that the treatment plan did not employ heterogeneity corrections, the differences between the measured and expected doses result from the metal magnet influence in the treatment deliveries. This approach was adopted because of the limited CT electron density calibration and poor modeling of the TPS algorithms for high Z

materials [5–9]. As can be seen, the measured dose was always higher than the planned one, as expected, due to the presence of the metallic prosthesis.

For the 6 MV beam irradiation, an overdose of 4.57% was achieved for all the films, and right above the magnet, an increase in dose of 11.22% was noticed. The increased dose within the casing of the metallic port for the 6 MV treatment is similar to the result found by Moni et al. [10]. This may occur due to differences in radiation scattering in this region, probably electrons produced in the interface. However, this hypothesis needs further studies, and it will be the subject of future research.

For the 15 MV beam irradiation, the films in the region around the magnet measured an overdose of 8.60% considering the planned value, and 5 mm away from the metal, we saw a decrease of 3.31% of the expected dose. It is known that laterally to the inhomogeneity, the electron fluence increases due to the increased lateral scattering from the material, producing an increased dose to the surrounding tissues [11]. However, the range of these electrons is limited, and a reduction in the dose was detected in film 4.

Our study detected different dose distribution patterns around the metallic implant for irradiations with different beam energies, which was expected due to the different radiation interactions that were not considered in the dose calculated by the treatment planning without heterogeneity correction [11]. The main interaction is the pair production occurring for the 15 MV beam and not for the 6 MV beam. The understanding of these effects is important not only for breast irradiation but can also contribute to other usual problems related to the presence of high Z materials in radiotherapy, such as pelvic irradiation in the presence of metallic femoral prosthesis [12] or the dosimetry using samples of tooth enamel [13].

It is important to cite that our study verified the dose distribution in the region perpendicular to the metallic implant, which is different from the most studies already presented in the literature that investigated the dosimetry of this treatment but looked at the radiation effects in the treatment beam directions [14–16]. They present almost a consensus from these studies that a radiation shadow occurs after the metal port dose with dose reductions.

4. CONCLUSION

The film measurements at the internal region of the prosthesis surrounding the metal showed a dose increase just above the magnet region for both energies. This hot spot region inside the prosthesis can be a problem if the metal is close to the surface of the saline prosthesis. A cold spot was observed only for the 15 MV beam at a 5 mm distance from the metal.

ACKNOWLEDGMENT

The authors thank Carlos Brunello and Lourenço Rocha for technical assistance. This work was supported by the Fundação de Amparo à Pesquisa do Estado de São Paulo (FAPESP) Grants 2013/03258-9, 2015/18221-9 & 2021/02254-6 and Conselho Nacional de Pesquisas e Desenvolvimento Tecnológico (CNPq) Grants 304107/2019-0 and Coordenação de Aperfeiçoamento de Pessoal de Nível Superior (CAPES) Finance Code 001.

REFERENCES

[1] Global Cancer Observatory: Cancer Today. Lyon, France: International Agency for Research on Cancer n.d. https://gco.iarc.fr/.

[2] Waks AG, Winer EP. Breast Cancer Treatment. JAMA 2019;321:288. https://doi.org/10.1001/jama.2018.19323.

[3] Asplund O, Körlof B. Late Results Following Mastectomy for Cancer and Breast Reconstruction. Scand J Plast Reconstr Surg 1984;18:221–5. https://doi.org/10.3109/02844318409052841.

[4] Kronowitz SJ, Robb GL. Radiation Therapy and Breast Reconstruction: A Critical Review of the Literature. Plast Reconstr Surg 2009;124:395–408. https://doi.org/10.1097/PRS.0b013e3181aee987.

[5] Acquah GF, Kyeremeh PO, Hasford F, Boadu M, Sosu EK, Inkoom S. Evaluation of metallic implant artifact on photon beam calculation algorithms using a CIRS thorax phantom. J

Radiat Res Appl Sci 2018;11:347–9. https://doi.org/10.1016/j.jrras.2018.06.005.

[6] Nakayama M, Yoshida K, Nishimura H, Miyawaki D, Uehara K, Okamoto Y, et al. Effect of heterogeneity correction on dosimetric parameters of radiotherapy planning for thoracic esophageal cancer. Med Dosim 2014;39:31–3. https://doi.org/10.1016/j.meddos.2013.09.001.

[7] Chen SA, Ogunleye T, Dhabbaan A, Huang EH, Losken A, Gabram S, et al. Impact of Internal Metallic Ports in Temporary Tissue Expanders on Postmastectomy Radiation Dose Distribution. Int J Radiat Oncol 2013;85:630–5. https://doi.org/10.1016/j.ijrobp.2012.06.046.

[8] Srivastava SP, Cheng C-W, Andrews J, Das IJ. Dose perturbation due to metallic breast expander in electron and photon beam treatment of breast cancer. J Radiat Oncol 2014;3:65–72. https://doi.org/10.1007/s13566-013-0109-4.

[9] Kairn T, Crowe SB, Fogg P, Trapp J V. The appearance and effects of metallic implants in CT images. Australas Phys Eng Sci Med 2013;36:209–17. https://doi.org/10.1007/s13246-013-0197-x.

[10] Moni J, Graves-Ditman M, Cederna P, Griffith K, Krueger EA, Fraass BA, et al. Dosimetry around metallic ports in tissue expanders in patients receiving postmastectomy radiation therapy: an ex vivo evaluation. Med Dosim 2004;29:49–54. https://doi.org/10.1016/j.meddos.2003.10.005.

[11] Reft C, Alecu R, Das IJ, Gerbi BJ, Keall P, Lief E, et al. Dosimetric considerations for patients with HIP prostheses undergoing pelvic irradiation. Report of the AAPM Radiation Therapy Committee Task Group 63. Med Phys 2003;30:1162–82. https://doi.org/10.1118/1.1565113.

[12] Rojas DMC, Pavoni JF, Arruda G V., Baffa O. Gel and thermoluminescence dosimetry for dose verifications of a real anatomy simulated prostate conformal radiation treatment in the presence of metallic femoral prosthesis. J Appl Clin Med Phys 2021;22:278–87. https://doi.org/10.1002/acm2.13403.

[13] Gómez JA, Marques T, Kinoshita A, Belmonte G, Nicolucci P, Baffa O. Influence of Dental Restorative Materials on ESR Biodosimetry in Tooth Enamel. Radiat Res 2011;176:259–63. https://doi.org/10.1667/RR2503.1.

[14] Thompson RCA, Morgan AM. Investigation into dosimetric effect of a MAGNA-SITE™ tissue expander on post-mastectomy radiotherapy. Med Phys 2005;32:1640–6.

https://doi.org/10.1118/1.1914545.

[15] Gee HE, Bignell F, Odgers D, Gill S, Martin D, Toohey J, et al. In vivo dosimetric impact of breast tissue expanders on post-mastectomy radiotherapy. J Med Imaging Radiat Oncol 2016;60:138–45. https://doi.org/10.1111/1754-9485.12403.

[16] da Silva MF, de Oliveira HF, Borges LF, Carrara HHA, Farina JA. Effects of the Metallic Port in Tissue Expanders on Dose Distribution in Postmastectomy Radiotherapy. Ann Plast Surg 2018;80:67–70. https://doi.org/10.1097/SAP.0000000000001177.